NHR-8 regulated P-glycoproteins uncouple xenobiotic stress resistance from longevity in chemosensory *C. elegans* mutants

Gabriel A. Guerrero[1], Klara Schilling[1], Felix A.M.C. Mayr[1], Ryan Lu[4], Bérénice A. Benayoun[4] & Martin S. Denzel[1,2,3]*

[1]Max Planck Institute for Biology of Ageing
Joseph-Stelzmann-Str. 9b
D-50931 Cologne, Germany

[2]CECAD - Cluster of Excellence
University of Cologne
Joseph-Stelzmann-Str. 26
D-50931 Cologne, Germany

[3]Center for Molecular Medicine Cologne (CMMC)
University of Cologne
Robert-Koch-Str. 21
D-50931 Cologne, Germany

[4]Leonard Davis School of Gerontology
University of Southern California
Los Angeles, CA 90089, USA

*correspondence:
mdenzel@age.mpg.de

Abstract

Longevity is often associated with stress resistance, but whether they are causally linked is incompletely understood. Here we investigate chemosensory defective *Caenorhabditis elegans* mutants that are long-lived and stress resistant. We find that mutants in the intraflagellar transport protein gene *osm-3* are completely protected from tunicamycin-induced ER stress. While *osm-3* lifespan extension is fully dependent on the key longevity factor DAF-16/FOXO, tunicamycin resistance is not. *osm-3* mutants are protected from bacterial pathogens, which is fully *pmk-1* p38 MAP kinase dependent. Transcriptomic analysis revealed enhanced expression of P-glycoprotein xenobiotic detoxification genes in *osm-3* mutants and chemical inhibition of P-glycoproteins with verapamil suppressed tunicamycin resistance. Of note, the nuclear hormone receptor *nhr-8* is necessary and sufficient to regulate P-glycoproteins and tunicamycin resistance. We thus identify a cell-nonautonomous regulation of xenobiotic detoxification and show that separate pathways are engaged to mediate longevity, pathogen resistance, and xenobiotic detoxification in *osm-3* mutants.

Introduction

Chemosensation is a genetically tractable phenotype in various model organisms. In *C. elegans*, many mutants with defective chemosensation have been identified. Sensory phenotypes are complex in nature and many of the classical chemosensory mutants were originally characterized by their behavioral phenotypes. Odr mutants for example have an abnormal odorant response while Osm (osmotic avoidance abnormal) mutants do not avoid high salt environments (Bargmann, 2006). In mutants like *tax-4* and *odr-1*, mutations in components of neuronal G-protein coupled receptor (GPCR) signaling cause atypical chemosensory behavior (Bargmann, 2006). These mutants are not only characterized by a failure to adequately respond to their environment, but show additional phenotypes linked to various life traits including pathogen resistance, increased lifespan and drug detoxification (Gaglia et al., 2012, Apfeld and Kenyon, 1999, Dent et al., 2000). Many chemosensory mutants are long lived and this phenotype depends on the DAF-16/FOXO transcription factor that is regulated by the insulin signaling pathway (Apfeld and Kenyon, 1999).

Beyond mutations in GPCRs, variants in genes involved in the development of amphid sensory neurons can lead to chemosensory defects. One example are mutations in intraflagellar transport (IFT) proteins that prevent full cilia development of amphid sensory neurons (Inglis et al., 2007). Alterations in the IFT genes *osm-3* and *daf-10* physically disrupt the development of neuronal dendrites that project toward the tip of the nose where they are exposed to the outer environment (Inglis et al., 2007). Thus, IFT mutants are usually characterized by defects in the chemical perception of their environment. Further, developmental defects in lumen formation of the amphid head channel in *daf-6* mutants prevent the direct contact of amphid sensory neurons with the outside (Perens and Shaham, 2005).

In wild type (WT) worms, amphid and phasmid sensory neurons can be visualized using the red lipophilic dye DiI, which fluorescently stains them bright red. The dye is passively taken up by sensory neurons when they are fully developed and in contact with the environment. Dye filling defective (Dyf) *C. elegans* are defined by an inability to take up DiI into their sensory neurons (Inglis et al., 2007). The Dyf phenotype arises in *daf-6* animals and also in many IFT mutants. Interestingly, Dyf mutants have unique stress resistance phenotypes that act via different signaling pathways. One such Dyf mutant, *daf-10(m79)*, has a unique resistance to pathogenic bacteria that was proposed to be downstream of sensory input (Gaglia et al., 2012). Further, pairs of amphid head neurons, such as ASH and ASJ that often become disrupted in Dyf mutants help coordinate the innate immune response to bacterial stress after infection (Meisel et al., 2014). Longevity is often associated with activation of physiological stress pathways and has been shown to be regulated by the insulin signaling pathway in Dyf *C. elegans* (Apfeld and Kenyon, 1999).

Conserved mechanisms of longevity and stress resistance have additionally been linked to hyposmia in higher model organisms. In *Drosophila melanogaster*, loss of the putative chemoreceptor *Or83b* has been shown to significantly increase lifespan (Libert et al., 2007). Further, mice with ablated olfactory sensory neurons, have a unique metabolic signature that protects them from high-fat diets (Riera et al., 2017).

While the olfactory machinery is seemingly more complex in higher organisms, *C. elegans* have unique phenotypes associated with the loss or alteration of their sensory neurons. First, unbiased screens for drug resistance have independently identified the Dyf phenotype as a common feature in drug resistant *C. elegans* (Fujii et al., 2004, Menez et al., 2016, Collins et al., 2008). Selection for resistance to the anthelmintic drug ivermectin was shown to enrich for Dyf mutants in several forward genetic screens (Menez et al., 2016, Page, 2018, Dent et al., 2000). Follow up work

identified P-glycoproteins, a class of ATP binding cassette (ABC) transporters, as the drivers behind ivermectin resistance in Dyf mutants (Ardelli and Prichard, 2013). Second, some chemosensory mutants, such as *daf-10*, show resistance to pathogenic bacteria (Gaglia et al., 2012).

Here, we characterize a long-lived Dyf mutant, *osm-3*, that was previously identified in a forward genetic screen for resistance to the potent ER stressor tunicamycin (TM). From this screen, we reported the role of the hexosamine biosynthetic pathway in TM resistance and longevity (Denzel et al., 2014). Our aim was to uncover the mechanism by which Dyf mutants are resistant to TM. Characterization of this phenotype demonstrates that TM resistance is independent from the *osm-3* longevity and pathogen resistance phenotypes. Further, using transcriptomics and functional analyses, we showed that P-glycoproteins mediate TM resistance in Dyf animals. In addition, we found that the nuclear hormone receptor *nhr-8* mediates *osm-3* drug resistance. Thus, our work highlights drug resistance as a unique characteristic of Dyf mutants and functionally uncouples it from known stress response pathways that have been implicated in stress resistance and longevity of chemosensory mutants.

Results

Dye filling defective *C. elegans* mutants are resistant to TM

TM is commonly used to induce endoplasmic reticulum (ER) stress by inhibiting the addition of N-glycans to nascent polypeptides (Parodi, 2000, Heifetz et al., 1979). In *C. elegans*, where the ER machinery is conserved, treatment with TM is toxic and induces the ER unfolded protein response. In fact, on plates containing TM at concentrations above 4 μg/mL, newly hatched larvae die at early developmental stages (Shen et al., 2001). Previously, we had carried out an ethyl methane-sulfonate (EMS) mutagenesis screen to identify TM resistant *C. elegans* (Denzel et al., 2014). The largest cohort of classifiable mutants presented dye filling defects (Dyf) (Figure 1A). Dyf mutants are uniquely characterized by their inability to take up the lipophilic red fluorescent dye DiI in their ciliated amphid neurons (Inglis et al., 2007).

Among the Dyf mutants from the TM resistance screen, we found new alleles of genes previously linked to ciliary development. The mutant allele we selected for our investigation, *osm-3(dh441) IV* (this allele will be referred to as *osm-3*), carries a premature stop in the third exon, which prevents normal cilia development causing the Dyf phenotype (Figure 1A, Supplementary Fig 1A;). *osm-3* is a member of the kinesin family involved in axonal transport and development and mutants are known to show a Dyf phenotype (Inglis et al., 2007). While WT worms fail to develop on TM at concentrations above 4 μg/mL, *osm-3* mutants fully develop at concentrations at least up to 10 μg/mL TM (Figure 1B). Loss of OSM-3, as well as other Dyf mutations, promotes longevity in *C. elegans* (Apfeld and Kenyon, 1999). Demographic lifespan analysis of *osm-3* indeed confirmed extended lifespan in our point mutant (Figure 1C and Supplementary Table 1). *osm-3* mutants, and Dyf mutants in general, have never been described as TM resistant especially at concentrations as high as 10 μg/mL.

To further explore whether the Dyf phenotype is linked to TM resistance we tested other Dyf mutants that were previously described as long lived in the literature (Apfeld and Kenyon, 1999). To our surprise, all Dyf mutants that we tested proved to be significantly TM resistant (Figure 1D, 1F). On the other hand, the long-lived chemosensory mutants *odr-1(n1936) X* and *odr-3(n2150) V* that display no Dyf phenotype were only slightly TM resistant (Figure 1E, 1F). Our data thus suggest that, among the larger class of chemosensory defective mutants, TM resistance is specifically found in Dyf mutants.

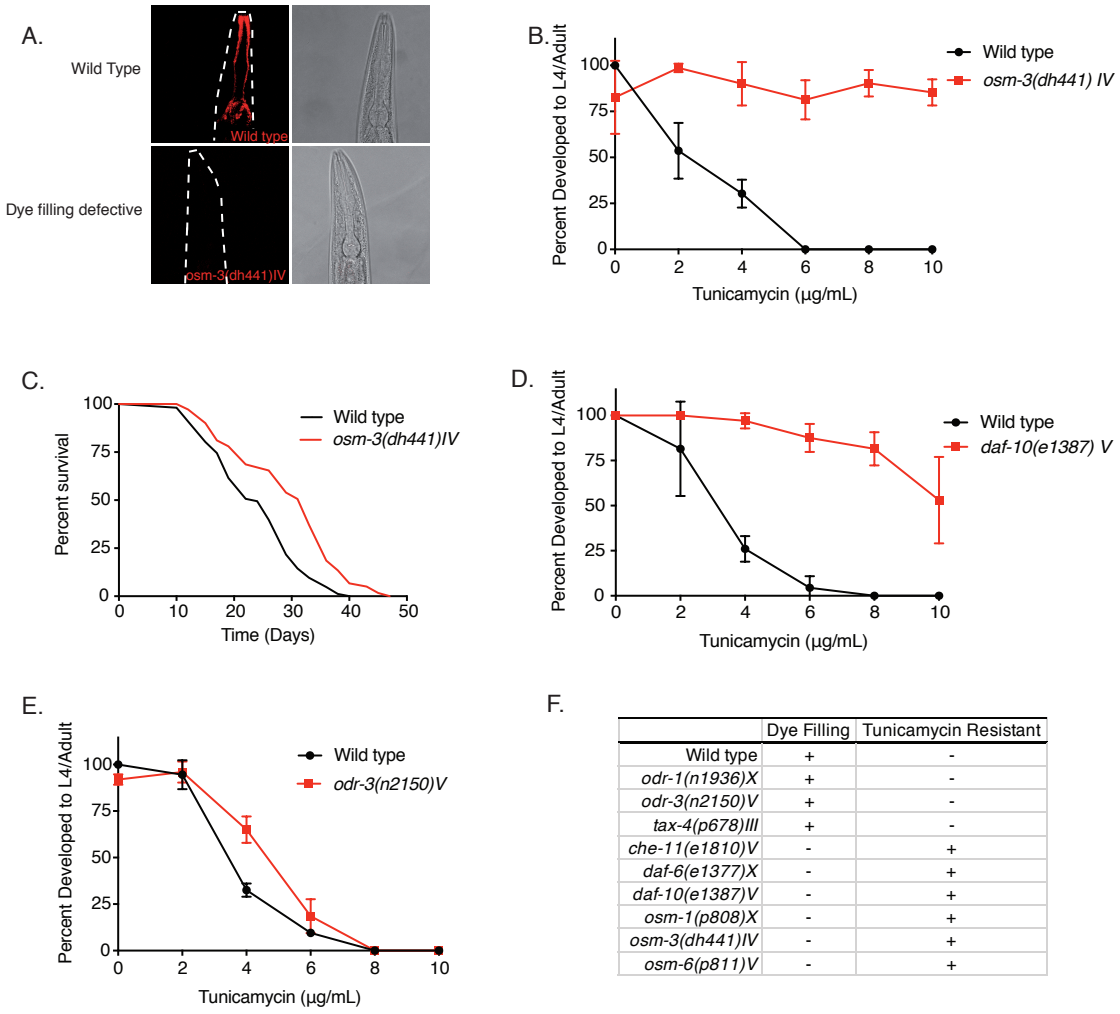

F.

	Dye Filling	Tunicamycin Resistant
Wild type	+	-
odr-1(n1936)X	+	-
odr-3(n2150)V	+	-
tax-4(p678)III	+	-
che-11(e1810)V	-	+
daf-6(e1377)X	-	+
daf-10(e1387)V	-	+
osm-1(p808)X	-	+
osm-3(dh441)IV	-	+
osm-6(p811)V	-	+

Figure 1. Dye filling defective *C. elegans* mutants are resistant to TM
A. Red fluorescence and differential interference contract confocal microscopy images of WT and *osm-3(dh441) IV C. elegans* after DiI treatment.
B. TM developmental assay with WT animals and *osm-3(dh441) IV* mutants.
C. Demographic lifespan analysis of WT and *osm-3(dh441) IV* animals. WT mean lifespan = 24 days, *osm-3(dh441) IV* mean lifespan = 29 days, $p < 0.0001$.
D. TM development assay with WT and *daf-10(e1387) V* mutants
E. TM development assay with WT and *odr-3(n2150) V* mutants
F. Table of dye filling phenotype and TM resistance. In the dye filling column, + is filled and - is Dyf. In the TM resistant column, + is resistant and - is not resistant to 10 µg/mL TM.

143

ER stress response is blunted in *osm-3* mutants

TM treatment activates the ER unfolded protein response (ER UPR); we thus characterized the overall transcriptional response of *osm-3* mutants upon TM treatment. We performed transcriptomic analysis on *osm-3* and WT worms after 6 hours of TM treatment. Notably, the gene ontology (GO) terms related to ER stress and ER protein folding showed significant upregulation in WT animals but not in *osm-3* mutants (Figure 2A). qPCR analysis of UPR target genes further confirmed that there was no ER UPR induction in the TM-treated *osm-3* mutants compared to the WT (Supplementary Figure 2). A hallmark of ER UPR induction in *C. elegans* is the upregulation of the molecular chaperone HSP-4/BiP (Shen et al., 2001). Upon TM treatment of *osm-3* mutants carrying a *hsp-4*::GFP reporter, there was no significant increase in the GFP signal compared to the untreated control, while in the WT the GFP levels were significantly increased (Figure 2A, 2B). This observation corroborates the results from the transcriptome analysis.

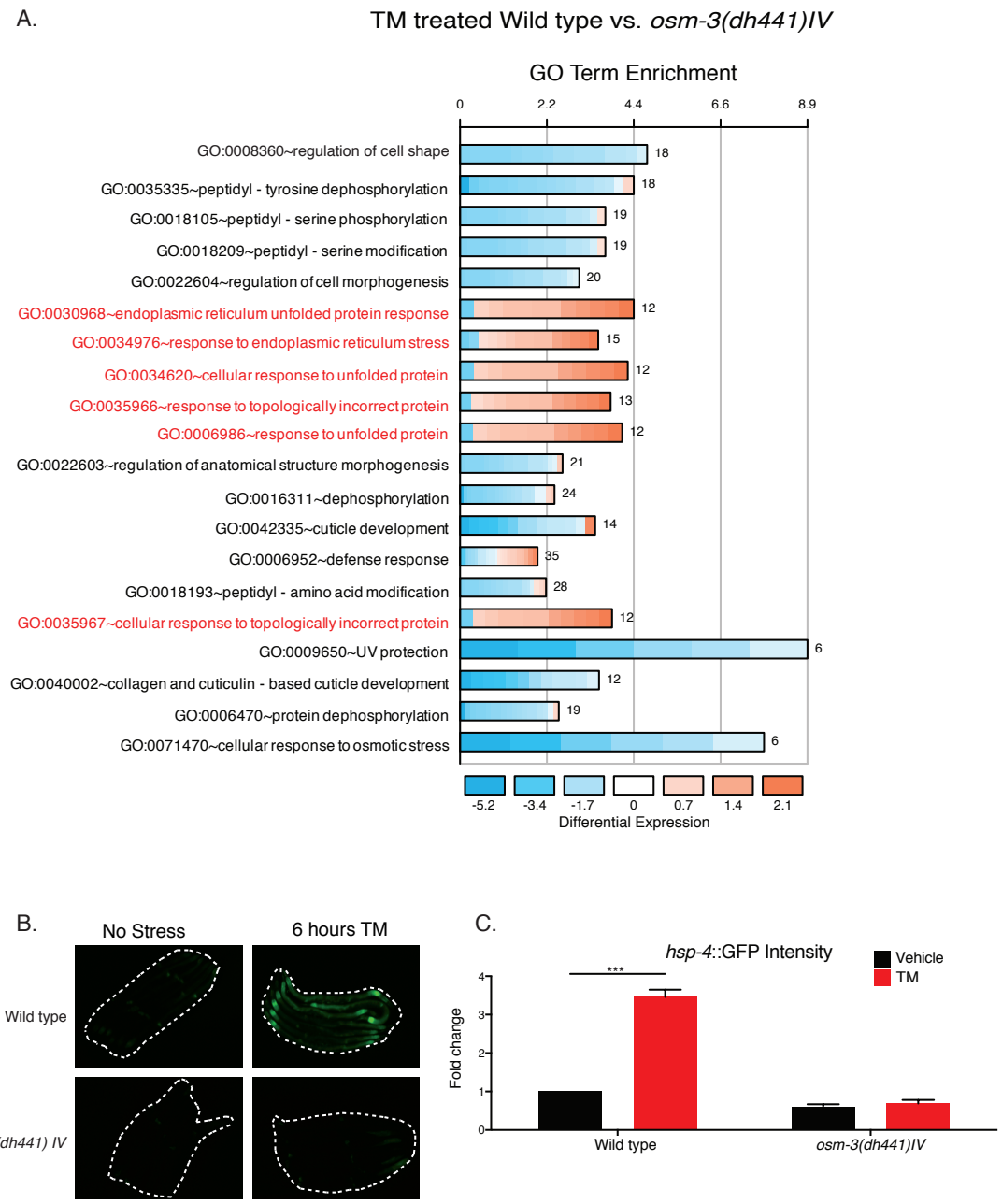

Figure 2. ER stress response is blunted in *osm-3* mutants
A. DAVID gene ontology (GO) terms that are enriched in TM-treated WT compared to TM-treated *osm-3(dh441) IV* worms. Red GO terms are upregulated and blue downregulated.
B. Green fluorescent images of WT and *osm-3(dh441) IV* animals in the *hsp-4*::GFP background after 6 hours of 10 μg/mL TM treatment. Worms are outlined in the images.
C. Biosorter analysis of *osm-3(dh441) IV* vs. WT animals in the *hsp-4*::GFP background after 6 hours of control or TM treatment. Data are mean + SEM, n = 4, *** p<0.0001 by two-way ANOVA.

158

TM resistance in *osm-3* mutants is not mediated through *daf-16* or PMK-1/p38 MAPK pathway

The lifespan extension observed in chemosensory defective *C. elegans* as well as in *Drosophila* has been shown to be at least partially insulin signaling dependent (Apfeld and Kenyon, 1999, Libert et al., 2007). Therefore, we performed a demographic lifespan analysis to determine the role of the insulin signaling pathway in the lifespan extension of *osm-3* mutants. Indeed, the *osm-3* lifespan extension was fully *daf-16* dependent, as the lifespan of the *osm-3; daf-16* double mutants was identical to the *daf-16* lifespan (Figure 3A and Supplementary Table 1). To our surprise, the *osm-3; daf-16* double mutant was resistant to TM while *daf-16* single mutants do not develop at 10 μg/mL TM (Figure 3B). Further, knock-down of *daf-16* by RNA interference did not rescue the *hsp-4*::GFP response after TM treatment (Figure 3C). Given previous links between the insulin signaling pathway and the ER stress signaling (Henis-Korenblit et al., 2010, Kyriakakis et al., 2017, Matai et al., 2019, Labbadia and Morimoto, 2014), we were surprised to find that *daf-2* mutants failed to develop on 10 μg/mL TM while *osm-3* mutants fully developed (Figure 3D). Together, this evidence suggests that the *osm-3* lifespan extension and TM drug resistance are uncoupled and instead appear to act via independent or parallel pathways.

In *C. elegans, Pseudomonas aeruginosa* PA14 is a pathogen that is often used to study innate immunity. Of note, ER UPR targets have been implicated in the innate immune response of *C. elegans* during PA14 infection (Richardson et al., 2010, Haskins et al., 2008). As the ER thus plays a role in innate immunity and as TM disrupts ER function, we speculated that *osm-3* mutants would be more robust on PA14 than WT. Indeed, *osm-3* mutants were more resistant to PA14 than WT, however this increased pathogen resistance was fully explained by the PMK-1 p38 mitogen-activated protein kinase (MAPK) pathway (Figure 3E). With this in mind, we tested

whether *pmk-1* mutation could suppress the *osm-3* TM resistance. The *osm-3; pmk-1* double mutant was fully resistant to TM, while the *pmk-1* single was fully sensitive (Figure 3F). Taken together, insulin signaling and the MAPK pathway, two major stress response pathways in *C. elegans* that have links to ER protein quality control, seemingly have no impact on *osm-3*'s TM resistance.

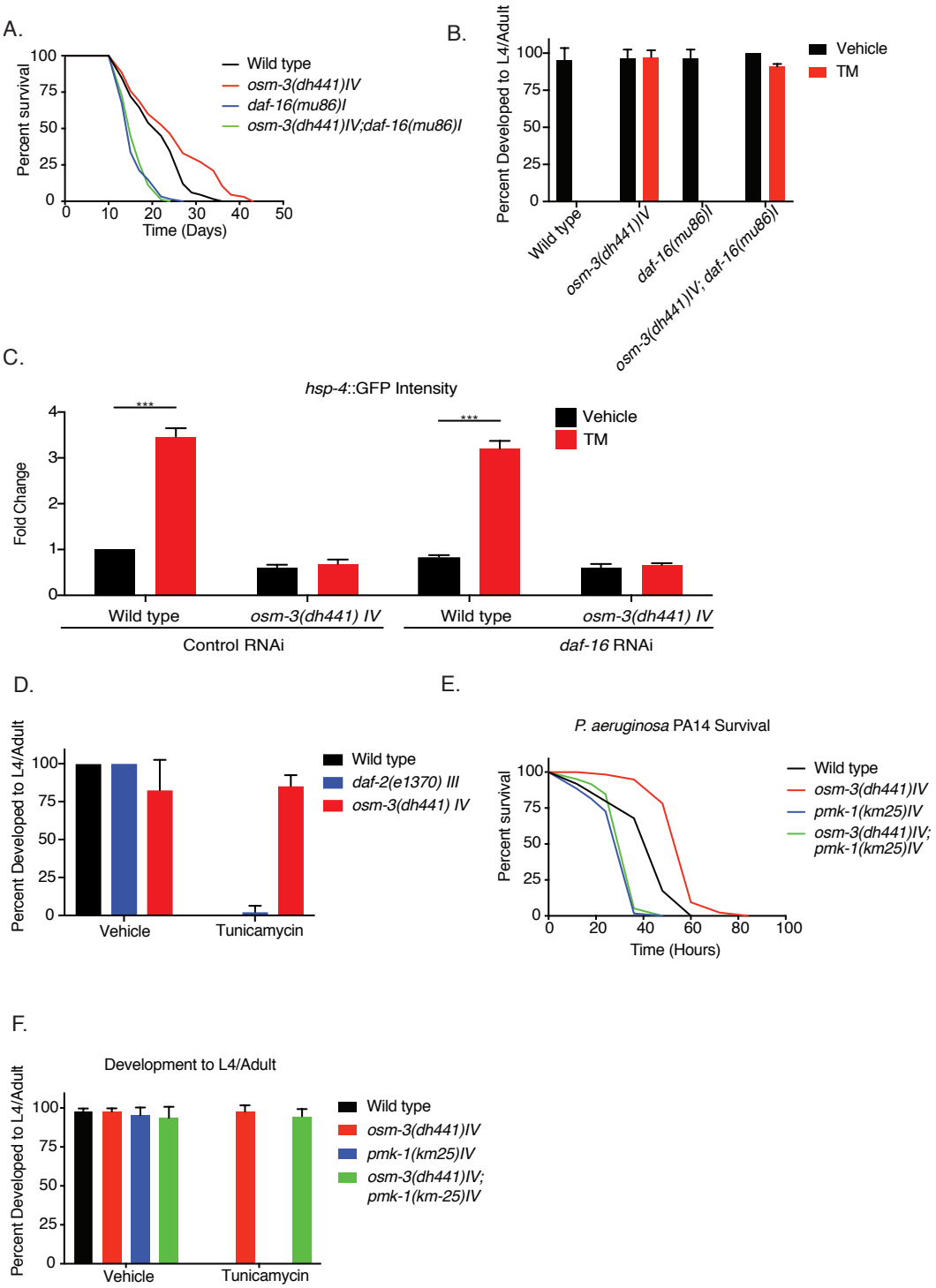

Figure 3. TM resistance in *osm-3* mutants is not *daf-16* or *pmk-1* dependent

A. Demographic lifespan analysis of WT, *osm-3(dhh441) IV*, *daf-16(mu86) I* and *osm-3(dh441) IV; daf-16(mu86) I* animals. WT mean lifespan = 22 days, *osm-3(dh441) IV* mean lifespan = 25 days $p < 0.005$ compared to WT, *daf-16(mu86) I* mean lifespan = 16 days $p < 0.0001$ compared to WT, *osm-3(dh441) IV*; *daf-16(mu86) I* mean lifespan = 16 days $p < 0.0001$ compared to WT.

B. TM developmental assay with WT, *osm-3(dh441) IV*, *daf-16(mu86) I*, and *osm-3(dh441) IV; daf-16(mu86) I* animals.

C. Biosorter analysis of *osm-3(dh441) IV* vs. WT in the *hsp-4*::GFP background raised on control or *daf-16* RNAi plates after 6 hours of control or TM treatment. Data are mean + SEM, n = 4, *** $p<0.001$ by two-way ANOVA.

D. TM developmental assay with WT, *osm-3(dh441) IV* and *daf-2(e1370) III* animals.

E. *Pseudomonas aeruginosa* PA14 survival assay with WT, *osm-3(dh441) IV*, *pmk-1(km25) IV*, and *osm-3(dh441) IV; pmk-1(km25) IV* animals. WT mean survival = 44 hours, *osm-3(dh441) IV* mean

survival = 58 hours p <0.001 compared to WT, *pmk-1(km25) IV* mean survival = 31 hours p <0.001 compared to WT, *osm-3(dh441) IV; pmk-1(km25) IV* mean survival = 34 hours p <0.001 compared to WT and p = 0.06 compared to *pmk-1(km25) IV*.
F. TM developmental assay with WT, *osm-3(dh441) IV*, *pmk-1(km25) IV*, and *osm-3(dh441) IV; pmk-1(km25) IV* animals.

P-glycoproteins are significantly enriched in *osm-3* mutants

The unique nature of Dyf drug resistance led us to investigate differences in overall gene expression under basal conditions. Our transcriptomic analysis revealed differential expression of P-glycoproteins (PGPs) in unstressed *osm-3* mutants compared to WT. Specifically, we found that the PGPs *pgp-2*, *pgp-4* and *pgp-14* were significantly upregulated in *osm-3* (Figure 4A). PGPs are a conserved family of ATP binding cassette (ABC) transporters found on the cell membrane (Sangster, 1994). *C. elegans* have 15 PGP genes. A comparison between control and TM treated WT and *osm-3* mutants showed no further enrichment of these PGPs upon TM treatment (Figure 4B). These findings led us to ask whether PGP upregulation is the driver of TM drug resistance in *C. elegans*.

P glycoprotein inhibition suppresses *osm-3* TM resistance

We tested whether elevated PGP expression might be responsible for the xenobiotic stress resistance in *osm-3* mutants. The PGP inhibitor verapamil (VPL) has been used to specifically inhibit PGP activity, re-sensitizing worms to the antihelmintic compound ivermectin (Menez et al., 2016). Indeed, 1 nM VPL significantly suppressed development of *osm-3 C. elegans* in the presence of TM, while having no effect on controls without TM (Figure 4C).

Dyf *C. elegans* mutants have been independently identified in drug resistance screens (Fujii et al., 2004, Menez et al., 2016, Dent et al., 2000). Consistent with these findings, we observed that *osm-3* mutants were resistant to 200 nM methyviologen dichloride (paraquat), as they fully develop at a concentration that is toxic to WT *C. elegans* (Figure 4D). Similarly, *osm-3* mutants fully developed to adults in the presence of 6 μg/mL ivermectin that is lethal to WT (Figure 4E). In contrast, *osm-3* mutants showed no difference to WT animals in heat stress assays or in the presence

of hydrogen peroxide (H_2O_2) suggesting that *osm-3* mutants are not resistant to non-xenobiotic stressors (Supplementary Figure 4A, 4B). Together, these observations suggest that *osm-3* mutants, and potentially Dyf mutants as a group, are significantly resistant to xenobiotic stress.

Having explained the TM resistance of *osm-3* mutants through PGP dependent xenobiotic detoxification, we wondered about its role in the longevity of *osm-3* mutants. Notably, VPL did not shorten *osm-3* lifespan. Moreover, VPL did not affect WT lifespan (Figure 4F and Supplementary Table 1) and had no visible effect on WT development (Supplementary Figure 4C). Together, these data support the conclusion that the xenobiotic stress resistance and longevity phenotypes of *osm-3* mutants are mediated by fully independent pathways.

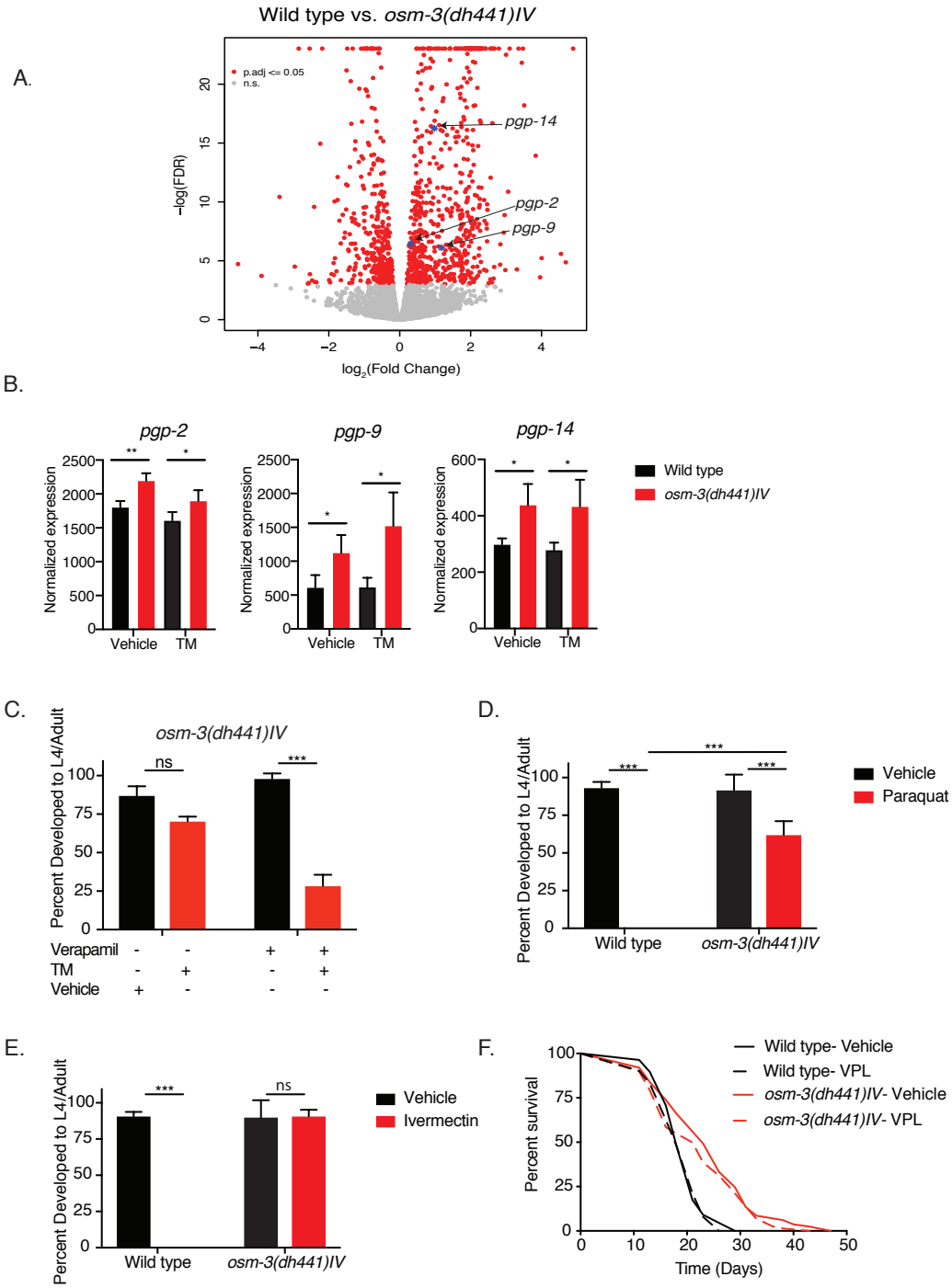

Figure 4. P-glycoproteins are significantly enriched in *osm-3* mutants

A. Volcano plot showing the global transcriptional changes in *osm-3(dh441) IV* compared to WT animals; *pgp-2*, *pgp-9* and *pgp-14* are labeled.

B. *pgp-2*, *pgp-9* and *pgp-14* expression levels in control and TM treated animals from transcriptomic data. Data are mean + SD, n = 4, * p<0.05, ** p<0.005 by t-test.

C. Verapamil (VPL) supplementation assay for development on TM using 10 μg/mL TM supplemented with vehicle or 1 nM VPL. Data are mean + SD, n = 3, *** p < 0.001 by two-way ANOVA.

D. Paraquat developmental assay of WT and *osm-3(dh441) IV* mutants using 0.2 mM paraquat and a vehicle control. Data are mean + SD, n = 3, *** p < 0.001 by two-way ANOVA.

E. Ivermectin developmental assay of WT and *osm-3(dh441) IV* mutants using 6 ng/mL ivermectin and a vehicle control. Data are mean + SD, n = 3, *** p < 0.001 by two-way ANOVA.

F. Demographic lifespan analysis on vehicle and VPL treated WT and *osm-3(dh441) IV* worms. Vehicle treated: WT mean lifespan = 19 days; *osm-3(dh441) IV* mean lifespan = 24 days p < 0.0001

compared to WT vehicle. VPL treated: WT mean lifespan = 19 days; *osm-3(dh441) IV* mean lifespan = 22 days, $p < 0.005$ compared to WT Vehicle.

NHR-8 signaling regulates xenobiotic detoxification response through PGPs

The nuclear hormone receptor NHR-8 has been linked to xenobiotic detoxification and PGP regulation in *C. elegans* (Menez et al., 2019, Lindblom et al., 2001). Indeed, using quantitative PCR we found that the upregulation of PGP expression in *osm-3* mutants was suppressed in the *osm-3; nhr-8* double mutant (Figure 5A). This led us to ask whether *osm-3* TM resistance was dependent on NHR-8 signaling. Indeed, the *osm-3; nhr-8(hd117) IV* double mutant was not resistant to TM while the *osm-3* mutant fully developed (Figure 5B), suggesting that NHR-8 is necessary for *osm-3* TM resistance. We next asked if NHR-8 is sufficient for TM resistance using a transgenic overexpressor line (Magner et al., 2013). Indeed, we found that overexpression of *nhr-8* in WT worms results in significant TM resistance (Figure 5C).

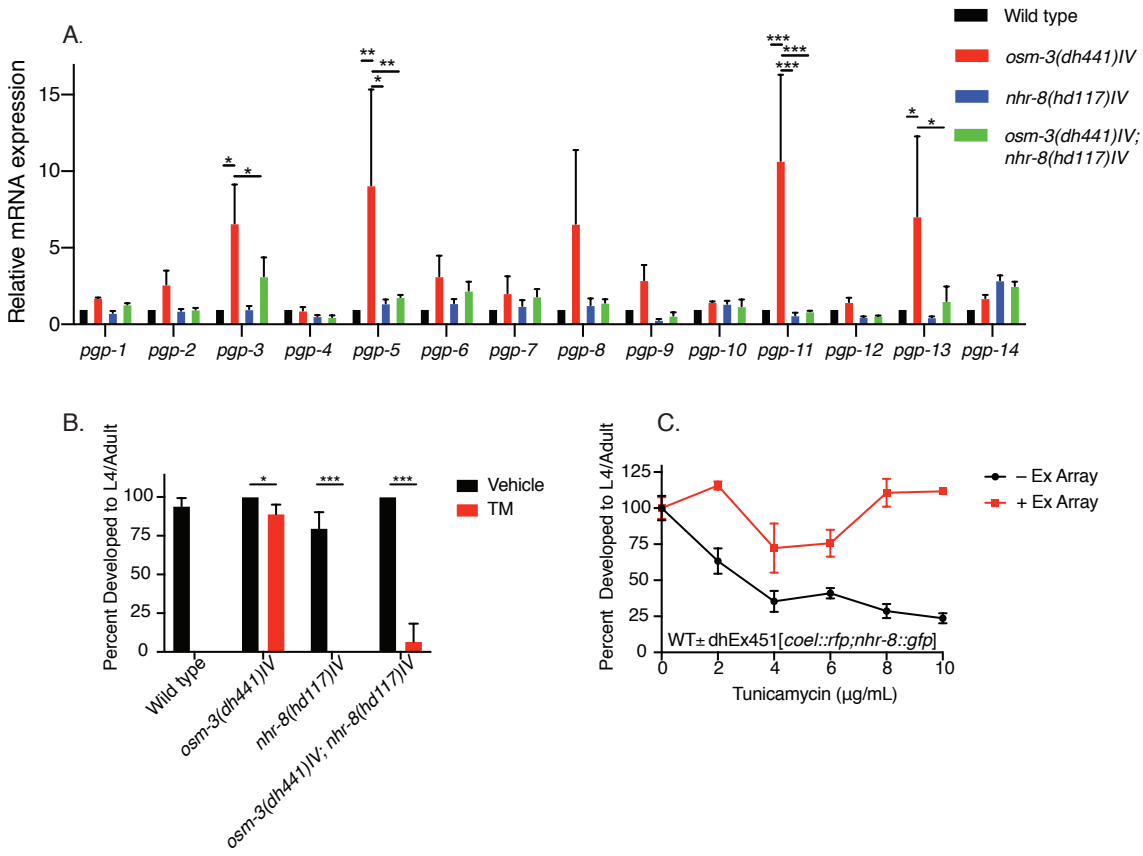

Figure 5. *nhr-8* signaling regulates xenobiotic detoxification response through PGPs

A. Quantitative PCR measuring relative PGP mRNA expression in WT, *osm-3(dh441) IV*, *nhr-8(hd117) IV* and *osm-3(dh441) IV; nhr-8(hd117) IV* animals. Data are mean + SEM, n = 3, * $p < 0.05$, ** $p < 0.001$, *** $p < 0.0001$ by two-way ANOVA.

B. TM developmental assay on 10 µg/mL TM and control with WT, *osm-3(dh441) IV*, *nhr-8(hd117) IV* and *osm-3(dh441) IV; nhr-8(hd117) IV* animals. Data are mean + SD, n = 3, * $p < 0.05$, *** $p < 0.0001$ by t-test.

C. TM developmental assay with transgenic animals containing an *nhr-8* overexpressing extrachromosomal array dhEx451[*coel::rfp;nhr-8::gfp*]. "-Ex Array" do not visibly contain the extrachromosomal array as judged by the co-injection marker and "+Ex Array" contain the extrachromosomal array. Data are mean + SEM, n = 3, * $p<0.05$ and *** $p < 0.005$ by two-way ANOVA.

241

Discussion

In this study, we found that Dyf mutants are resistant to the ER toxin TM. Instead of an activated stress signaling status that might explain the TM resistance, *osm-3* Dyf mutants show no ER UPR induction upon TM treatment. Consistent with previous findings (Apfeld and Kenyon, 1999) the lifespan extension of *osm-3* was *daf-16* dependent. Despite the established link between the insulin signaling pathway and stress resistance, the TM resistance in *osm-3* mutants was not insulin signaling dependent. Further, while *osm-3* mutants were pathogen resistant, this resistance was fully dependent on the PMK-1/p38 MAPK pathway. We were surprised that neither of the two pathways weakened the TM resistance phenotype. Dyf *C. elegans* drug resistance is not specific to TM, as we also observed resistance to paraquat and ivermectin. While paraquat and ivermectin resistance have been previously reported in Dyf mutants (Dent et al., 2000, Fujii et al., 2004, Menez et al., 2016), no studies have demonstrated similar resistance mechanisms in Dyf *C. elegans* mutants to TM. Our findings show that this resistance is due to increased PGP expression in Dyf worms. Importantly, we demonstrate regulation of PGPs by the nuclear hormone receptor NHR-8. Broad inhibition of PGPs using verapamil or loss of *nhr-8* significantly resensitized *osm-3* mutants to TM. Consistently, NHR-8 overexpression resulted in TM resistance in WT animals. These data show that *nhr-8* is necessary and sufficient for TM resistance.

Given that improved protein homeostasis is one of the cellular hallmarks of longevity (Lopez-Otin et al., 2013), we presumed that selection for TM resistance would serve as a proxy phenotype for longevity given that TM specifically targets ER protein folding. More specifically, we expected that high fidelity ER protein quality control would be the driver of longevity in these mutants. Previous findings describing increased hexosamine biosynthetic pathway flux (Denzel et al., 2014) or constitutive

XBP-1 activation (Taylor and Dillin, 2013) have linked protein homeostasis to longevity and stress resistance; therefore the connection between TM resistance and longevity seemed apparent. Given that Dyf mutants are resistant to pathogenic bacteria through enhanced ER homeostasis, we also speculated that TM resistance might serve as a proxy phenotype for pathogen resistance. On the contrary, we found that increased PGP expression is sufficient to drive detoxification in TM resistance but not longevity in *osm-3* mutants. *pmk-1* and *daf-16* were behind pathogen resistance and longevity, respectively.

Adding another dimension to the cell-nonautonomous regulation of innate immunity (Aballay, 2013), we propose that the nervous system regulates systemic xenobiotic detoxification *C. elegans*. Our data suggest that mutants with defective amphid neurons have increased PGP expression. Several PGPs have been shown to be expressed in non-neuronal tissue (Lincke et al., 1993, Sheps et al., 2004). Moreover, we found that PGP expression is regulated by *nhr-8*, which has also been shown to be expressed in the intestine of *C. elegans* (Magner et al., 2013). Combining this previous information with our finding that Dyf mutants are resistant to several uniquely toxic drugs, we conclude that neuronal signaling controls drug resistance through nuclear hormone signaling. To this end one might further investigate the link between neuronal states and the cholesterol-derived signal that drives these drug resistance phenotypes.

PGPs are likely regulated in *C. elegans* to help them combat toxins found in their natural habitat. Toxic metabolites are undoubtedly common in the soil where *C. elegans* are found. The drugs used in our study, ivermectin (a derivative of avermectin) (Burg et al., 1979) and TM, were first discovered as antibiotics that are produced by soil bacteria (Takatsuki et al., 1971). Because *C. elegans* have no adaptive immune response, having PGPs as part of their innate immune system allows

294 them to clear toxic molecules they may encounter in the wild. While Dyf mutants do
295 not occur in the wild, our data nonetheless demonstrate a link environmental sensing
296 and drug resistance.

297 In humans, PGPs have been implicated in drug resistant malignancies (Lehne,
298 2000). Using *C. elegans* as a tool to study the cross talk between tissues, one might
299 be able to better understand how extracellular signaling drives ABC transporter
300 expression in chemotherapy resistant cancer. Further studies in cell culture might also
301 further characterize TM, as well as other toxic metabolites, as substrates for *C. elegans*
302 PGPs.

Materials and Methods

Worm maintenance

C. elegans nematodes were cultured using standard husbandry methods at 20°C on nematode growth media (NGM) agar plates seeded with *E. coli* strain OP50 unless otherwise stated (Brenner, 1974).

Dye filling assay in *C. elegans*

The dye filling assay was performed on a synchronized population of day 1 adults. 40-60 adult worms were placed in M9 containing 10 μg/mL DiI. They were left at room temperature for two hours in the staining medium, then transferred to NGM plates seeded with *E. coli* OP50. The worms were then allowed to crawl on the food for one hour to allow for the dye to be cleared from the gut. The worms were scored for dye filling using a Leica SPX-8 confocal microscope or a Leica fluorescent stereo-microscope. Images were taken using the confocal microscope.

Drug resistance assays

NGM plates containing either TM, paraquat or ivermectin were used in developmental assays to test for resistance. To this end, we performed a 4h egg lay on NGM plates at room temperature then transferred the eggs to control and drug containing plates and recorded the number of eggs per plate. After incubation for four days at 20°C, plates were scored by counting the total number of L4 larvae or adults on each plate. Paraquat plates were prepared by adding 1M methyl viologen dichloride (paraquat) directly onto seeded NGM plates for a final concentration of 200 μM and allowed to dry immediately before use. Ivermectin plates were prepared by adding ivermectin directly to the NGM medium at a final concentration of 6 μg/mL before

pouring the plates. Modified NGM plates containing no cholesterol were made by using standard NGM without the addition of cholesterol. These modified NGM plates were then supplemented with drugs as described above. All of the drug development assays were performed using *E. coli* OP50 bacteria.

ER stress quantification by *hsp-4*::GFP

Synchronized day 1 adults were transferred to control and TM containing NGM plates seeded with OP50. After 6 hours of stress induction *hsp-4*::GFP levels were measured by large particle flow cytometry in both the WT and *osm-3(dh441)IV* background using the Union Biometrica Biosorter. For *daf-16* knockdown by RNAi, animals were raised on control and *daf-16* RNAi. Synchronized day 1 adults were transferred to control or TM containing plates seeded with control or *daf-16* RNAi. After 6 hours of stress, GFP levels were measured using the Biosorter. GFP values were normalized to time of flight.

Quantitative PCR

For ER stress induction day 1 adults were washed from their plates and transferred to either control or TM containing plates, where they were incubated for 6h. The animals were then washed off using M9 and snap frozen in trizol. Unstressed synchronized animals were collected at day 1 of adult hood for RNA extraction. RNA was prepared using Zymo Research Direct-zol RNA Microprep kit. SYBR green was used to perform quantitative PCR (RT-qPCR). See Supplementary Materials for list of qPCR primers used in this study.

352 **Lifespan analysis**

353 Adult lifespan analysis was performed at 20°C on mutant and WT *C. elegans*.
354 The animals were synchronized in a four-hour egg lay. Animals were scored as dead
355 or alive every second day until the end of the experiment. Animals were transferred
356 every day for the first seven days. Statistical analysis on the Kaplan-Meier survival
357 curves was performed using Microsoft Excel. See Supplementary Materials for lifespan
358 statistics.

359

360 **Hydrogen peroxide survival assay**

361 1M hydrogen peroxide (H_2O_2) was added to unseeded NGM plates to a final
362 concentration of 1 μM and allowed to dry for several minutes. Synchronized day one
363 adults were then transferred onto the plates and incubated at 25°C. The animals were
364 then scored every 2 hours for survival.

365

366 **Pathogenic bacteria survival assay**

367 The *Pseudomonas aeruginosa* strain PA14 was grown in LB media and seeded
368 onto high peptone NGM plates and incubated for 12 hours at 37°C immediately before
369 the start of the experiment. Day one animals were first transferred to unseeded NGM
370 plates to crawl around the plate and remove any excess *E. coli* OP50 off of their bodies.
371 They were then transferred to the PA14 containing plates and incubated at 25°C. The
372 animals were scored every 12 hours until all animals were dead.

373

374 **Heat stress survival assay**

375 Day 1 synchronized *C. elegans* were transferred to fresh NGM plates seeded
376 with *E. coli* OP50. These plates were transferred to a 35°C incubator, where they were

377 evenly distributed throughout the incubator to ensure even heat exposure. The plates
378 were scored for live worms every 2 hours until all of the worms were dead.
379
380 **Sample collection and RNA purification for sequencing**
381 For RNA sequencing we used day one adults that were hatched within one hour.
382 To achieve this synchronization, we washed all adults and larvae of plates with M9 and
383 allowed the eggs on hatch for one hour. The freshly hatched L1 larvae were then
384 washed off and transferred to fresh plates seeded with OP50 and incubated at 20°C
385 until they developed to adults. At day one of adulthood, animals were washed from
386 their plates and transferred to either control or TM containing plates, where they were
387 incubated for 6 hours. The animals were then washed off using M9 and snap frozen in
388 trizol. All biological replicates were collected and prepared using a snaking collection
389 method to reduce batch effects. Total RNA was purified using Zymo Research Direct-
390 zol RNA Microprep kit.
391
392 **RNA-seq library preparation**
393 RNA quality was assessed using Agilent's Bioanalyzer platform, and samples
394 with RIN > 9 were used for library construction. 2.5 µg of total RNA was subjected to
395 ribosomal RNA (rRNA) depletion using the Illumina's Ribo-zero Gold kit (Illumina),
396 according to the manufacturer's protocol. Strand specific RNA-seq libraries were then
397 constructed using the SMARTer Stranded RNA-Seq HT Kit (Clontech #634839),
398 according to the manufacturer's protocol. Based on rRNA-depleted input amount, 15
399 cycles of amplification were performed to generate RNA-seq libraries. Paired-end
400 150 bp reads were sent for sequencing on the Illumina HiSeq-Xten platform at the
401 Novogene Corporation (USA). The resulting data was then analyzed with a
402 standardized RNA-seq data analysis pipeline (described below).

403 **RNA-seq analysis pipeline**

404 cDNA sequences of worm genes were obtained through ENSEMBL Biomart for
405 the WBCel235 build of the *C. elegans* genome (Ensemble release v94; accessed
406 2018-12-03). Trimmed reads were mapped to this reference using kallisto 0.43.0-1 and
407 the –fr-stranded option (Bray et al., 2016). All subsequent analyses were performed in
408 the R statistical software (https://cran.r-project.org/). Read counts were imported into
409 R, and summarized at the gene level. Differential gene expression was estimated using
410 the 'DESeq2' R package (DESeq2 1.16.1) [PMID: 25516281]. David analysis (version
411 6.8) was performed to identify significantly enriched gene ontology terms.

412

413 **Developmental verapamil (VPL) resistance assay and lifespan analysis**

414 Plates containing 10 μg/mL TM were supplemented with 1 nM VPL by adding
415 VPL solved in DMSO onto the plates. Plates were allowed to dry for 6h before eggs
416 were transferred to them to determine developmental resistance to TM. Plates were
417 then scored after 4 days to determine the relative number of L4 larvae or adults.
418 Lifespan assays were performed as above, however the animals were transferred to
419 fresh VPL containing plates every second day for the whole lifespan assay.

Acknowledgements

We thank all M.S.D. laboratory members for lively and helpful discussions. We thank Adam Antebi for valuable comments and for *C. elegans* strains. We thank Seung-Jae Lee for valuable comments on the manuscript. We thank the Caenorhabditis Genetics Center (CGC) for strains. We thank the members of the bioinformatics core facility and the FACS and imaging core facility at MPI AGE. B.A.B is supported by a seed grant from the NAVIGAGE foundation, and a generous gift from the Hanson-Thorell Family. M.S.D. was supported by ERC-StG 640254, by the Deutsche Forschungsgemeinschaft (DFG, German Research Foundation) - Projektnummer 73111208 - SFB 829, and by the Max Planck Society.

Competing interests

The authors declare no competing interests.

References

ABALLAY, A. 2013. Role of the nervous system in the control of proteostasis during innate immune activation: insights from C. elegans. *PLoS Pathog,* 9**,** e1003433.

APFELD, J. & KENYON, C. 1999. Regulation of lifespan by sensory perception in Caenorhabditis elegans. *Nature,* 402**,** 804-9.

ARDELLI, B. F. & PRICHARD, R. K. 2013. Inhibition of P-glycoprotein enhances sensitivity of Caenorhabditis elegans to ivermectin. *Vet Parasitol,* 191**,** 264-75.

BARGMANN, C. I. 2006. Chemosensation in C. elegans. *WormBook***,** 1-29.

BRAY, N. L., PIMENTEL, H., MELSTED, P. & PACHTER, L. 2016. Near-optimal probabilistic RNA-seq quantification. *Nat Biotechnol,* 34**,** 525-7.

BRENNER, S. 1974. The genetics of Caenorhabditis elegans. *Genetics,* 77**,** 71-94.

BURG, R. W., MILLER, B. M., BAKER, E. E., BIRNBAUM, J., CURRIE, S. A., HARTMAN, R., KONG, Y. L., MONAGHAN, R. L., OLSON, G., PUTTER, I., TUNAC, J. B., WALLICK, H., STAPLEY, E. O., OIWA, R. & OMURA, S. 1979. Avermectins, new family of potent anthelmintic agents: producing organism and fermentation. *Antimicrob Agents Chemother,* 15**,** 361-7.

COLLINS, J. J., EVASON, K., PICKETT, C. L., SCHNEIDER, D. L. & KORNFELD, K. 2008. The anticonvulsant ethosuximide disrupts sensory function to extend C. elegans lifespan. *PLoS Genet,* 4**,** e1000230.

DENT, J. A., SMITH, M. M., VASSILATIS, D. K. & AVERY, L. 2000. The genetics of ivermectin resistance in Caenorhabditis elegans. *Proc Natl Acad Sci U S A,* 97**,** 2674-9.

DENZEL, M. S., STORM, N. J., GUTSCHMIDT, A., BADDI, R., HINZE, Y., JAROSCH, E., SOMMER, T., HOPPE, T. & ANTEBI, A. 2014. Hexosamine pathway metabolites enhance protein quality control and prolong life. *Cell,* 156**,** 1167-1178.

FUJII, M., MATSUMOTO, Y., TANAKA, N., MIKI, K., SUZUKI, T., ISHII, N. & AYUSAWA, D. 2004. Mutations in chemosensory cilia cause resistance to paraquat in nematode Caenorhabditis elegans. *J Biol Chem,* 279**,** 20277-82.

GAGLIA, M. M., JEONG, D. E., RYU, E. A., LEE, D., KENYON, C. & LEE, S. J. 2012. Genes that act downstream of sensory neurons to influence longevity, dauer formation, and pathogen responses in Caenorhabditis elegans. *PLoS Genet,* 8**,** e1003133.

HASKINS, K. A., RUSSELL, J. F., GADDIS, N., DRESSMAN, H. K. & ABALLAY, A. 2008. Unfolded protein response genes regulated by CED-1 are required for Caenorhabditis elegans innate immunity. *Dev Cell,* 15**,** 87-97.

HEIFETZ, A., KEENAN, R. W. & ELBEIN, A. D. 1979. Mechanism of action of tunicamycin on the UDP-GlcNAc:dolichyl-phosphate Glc-NAc-1-phosphate transferase. *Biochemistry,* 18**,** 2186-92.

HENIS-KORENBLIT, S., ZHANG, P., HANSEN, M., MCCORMICK, M., LEE, S. J., CARY, M. & KENYON, C. 2010. Insulin/IGF-1 signaling mutants reprogram ER stress response regulators to promote longevity. *Proc Natl Acad Sci U S A,* 107**,** 9730-5.

INGLIS, P. N., OU, G., LEROUX, M. R. & SCHOLEY, J. M. 2007. The sensory cilia of Caenorhabditis elegans. *WormBook***,** 1-22.

KYRIAKAKIS, E., CHARMPILAS, N. & TAVERNARAKIS, N. 2017. Differential adiponectin signalling couples ER stress with lipid metabolism to modulate ageing in C. elegans. *Sci Rep,* 7**,** 5115.

LABBADIA, J. & MORIMOTO, R. I. 2014. Proteostasis and longevity: when does aging really begin? *F1000Prime Rep,* 6**,** 7.

LEHNE, G. 2000. P-glycoprotein as a drug target in the treatment of multidrug resistant cancer. *Curr Drug Targets,* 1**,** 85-99.

LIBERT, S., ZWIENER, J., CHU, X., VANVOORHIES, W., ROMAN, G. & PLETCHER, S. D. 2007. Regulation of Drosophila life span by olfaction and food-derived odors. *Science,* 315**,** 1133-7.

LINCKE, C. R., BROEKS, A., THE, I., PLASTERK, R. H. & BORST, P. 1993. The expression of two P-glycoprotein (pgp) genes in transgenic Caenorhabditis elegans is confined to intestinal cells. *EMBO J,* 12**,** 1615-20.

LINDBLOM, T. H., PIERCE, G. J. & SLUDER, A. E. 2001. A C. elegans orphan nuclear receptor contributes to xenobiotic resistance. *Curr Biol,* 11**,** 864-8.

LOPEZ-OTIN, C., BLASCO, M. A., PARTRIDGE, L., SERRANO, M. & KROEMER, G. 2013. The hallmarks of aging. *Cell,* 153**,** 1194-217.

MAGNER, D. B., WOLLAM, J., SHEN, Y., HOPPE, C., LI, D., LATZA, C., ROTTIERS, V., HUTTER, H. & ANTEBI, A. 2013. The NHR-8 nuclear receptor regulates cholesterol and bile acid homeostasis in C. elegans. *Cell Metab,* 18**,** 212-24.

MATAI, L., SARKAR, G. C., CHAMOLI, M., MALIK, Y., KUMAR, S. S., RAUTELA, U., JANA, N. R., CHAKRABORTY, K. & MUKHOPADHYAY, A. 2019. Dietary restriction improves proteostasis and increases life span through endoplasmic reticulum hormesis. *Proc Natl Acad Sci U S A,* 116**,** 17383-17392.

MEISEL, J. D., PANDA, O., MAHANTI, P., SCHROEDER, F. C. & KIM, D. H. 2014. Chemosensation of bacterial secondary metabolites modulates neuroendocrine signaling and behavior of C. elegans. *Cell,* 159**,** 267-80.

MENEZ, C., ALBERICH, M., COURTOT, E., GUEGNARD, F., BLANCHARD, A., AGUILANIU, H. & LESPINE, A. 2019. The transcription factor NHR-8: A new target to increase ivermectin efficacy in nematodes. *PLoS Pathog,* 15**,** e1007598.

MENEZ, C., ALBERICH, M., KANSOH, D., BLANCHARD, A. & LESPINE, A. 2016. Acquired Tolerance to Ivermectin and Moxidectin after Drug Selection Pressure in the Nematode Caenorhabditis elegans. *Antimicrob Agents Chemother,* 60**,** 4809-19.

PAGE, A. P. 2018. The sensory amphidial structures of Caenorhabditis elegans are involved in macrocyclic lactone uptake and anthelmintic resistance. *Int J Parasitol,* 48**,** 1035-1042.

PARODI, A. J. 2000. Role of N-oligosaccharide endoplasmic reticulum processing reactions in glycoprotein folding and degradation. *Biochem J,* 348 Pt 1**,** 1-13.

PERENS, E. A. & SHAHAM, S. 2005. C. elegans daf-6 encodes a patched-related protein required for lumen formation. *Dev Cell,* 8**,** 893-906.

RICHARDSON, C. E., KOOISTRA, T. & KIM, D. H. 2010. An essential role for XBP-1 in host protection against immune activation in C. elegans. *Nature,* 463**,** 1092-5.

RIERA, C. E., TSAOUSIDOU, E., HALLORAN, J., FOLLETT, P., HAHN, O., PEREIRA, M. M. A., RUUD, L. E., ALBER, J., THARP, K., ANDERSON, C. M., BRONNEKE, H., HAMPEL, B., FILHO, C. D. M., STAHL, A., BRUNING, J. C. & DILLIN, A. 2017. The Sense of Smell Impacts Metabolic Health and Obesity. *Cell Metab,* 26**,** 198-211 e5.

SANGSTER, N. C. 1994. P-glycoproteins in nematodes. *Parasitol Today,* 10**,** 319-22.

SHEN, X., ELLIS, R. E., LEE, K., LIU, C. Y., YANG, K., SOLOMON, A., YOSHIDA, H., MORIMOTO, R., KURNIT, D. M., MORI, K. & KAUFMAN, R. J. 2001. Complementary signaling pathways regulate the unfolded protein response and are required for C. elegans development. *Cell,* 107**,** 893-903.

525 SHEPS, J. A., RALPH, S., ZHAO, Z., BAILLIE, D. L. & LING, V. 2004. The ABC transporter gene
526 family of Caenorhabditis elegans has implications for the evolutionary dynamics of
527 multidrug resistance in eukaryotes. *Genome Biol,* 5**,** R15.
528 TAKATSUKI, A., ARIMA, K. & TAMURA, G. 1971. Tunicamycin, a new antibiotic. I. Isolation
529 and characterization of tunicamycin. *J Antibiot (Tokyo),* 24**,** 215-23.
530 TAYLOR, R. C. & DILLIN, A. 2013. XBP-1 is a cell-nonautonomous regulator of stress
531 resistance and longevity. *Cell,* 153**,** 1435-47.
532